Model-Based Inference and Classification of Immunologic Control Mechanisms from TKI Cessation and Dose Reduction in Patients with CML

Hähnel, Tom

2020-06-01

Hähnel , T , Baldow , C , Guilhot , J , Guilhot , F , Saussele , S , Mustjoki , S , Jilg , S , Jost , P J , Dulucq , S , Mahon , F-X , Roeder , I , Fassoni , A C & Glauche , I 2020 , ' Model-Based Inference and Classification of Immunologic Control Mechanisms from TKI Cessation and Dose Reduction in Patients with CML ' , Cancer Research , vol. 80 , no. 11 , pp. 2394-2406 . https://doi.org/10.1158/0008-5472.CAN-19-2175

http://hdl.handle.net/10138/331937
https://doi.org/10.1158/0008-5472.CAN-19-2175

acceptedVersion

Model-based inference and classification of immunological control mechanisms from TKI cessation and dose reduction in CML patients

Tom Hähnel[1], Christoph Baldow[1], Joëlle Guilhot[2], François Guilhot[2], Susanne Saussele[3], Satu Mustjoki[4,5], Stefanie Jilg[6], Philipp J. Jost[6], Stephanie Dulucq[7], François-Xavier Mahon[8], Ingo Roeder[1,9], Artur C. Fassoni[10 *], Ingmar Glauche[1 *]

[1] Institute for Medical Informatics and Biometry, Carl Gustav Carus Faculty of Medicine, Technische Universität Dresden, Germany
[2] INSERM CIC 1402 - CHU Poitiers, France
[3] III. Medizinische Klinik, Universitätsmedizin Mannheim, Heidelberg University, Germany
[4] Hematology Research Unit Helsinki, Helsinki University Hospital Comprehensive Cancer Center, Helsinki, Finland
[5] Translational Immunology Research Program and Department of Clinical Chemistry and Hematology, University of Helsinki, Helsinki, Finland
[6] III. Medizinische Klinik und Poliklinik, Klinikum rechts der Isar, Technische Universität München, Germany
[7] Laboratory of Hematology , University Hospital of Bordeaux, France
[8] Bergonie institute, INSERM U1218 University of Bordeaux, France
[9] National Center for Tumor Diseases (NCT), Partner Site Dresden, Germany
[10] Instituto de Matemática e Computação, Universidade Federal de Itajubá, Brazil

* these authors contributed equally

Running title: Inferring immunological control mechanisms in CML patients

Keywords: CML, immunological control, tyrosine kinase inhibitor, treatment stop, dose reduction, mathematical modelling

Corresponding author:
Ingmar Glauche
Institute for Medical Informatics and Biometry
Faculty of Medicine Carl Gustav Carus, Technical University Dresden
Fetscherstrasse. 74, D-01307 Dresden
phone: +49 (0) 351 458 6051, fax: +49 (0) 351 458 7222
email: ingmar.glauche@tu-dresden.de

abstract word count: 242
word count: 5386 / 5000
number of figures: 7

Financial support: This work was supported by the German Federal Ministry of Education and Research (www.bmbf.de/en/), Grant number 031A424 “HaematoOpt” to IR and Grant number 031A315 “MessAge” to IG, as well as the ERA-Net ERACoSysMed JTC-2 project “prediCt” (project number 031L0136A) to IR. The research of ACF was supported by the Excellence Initiative of the German Federal and State Governments (Dresden Junior Fellowship) and by CAPES/Pós-Doutorado no Exterior Grant number 88881.119037/2016-01. SM was supported by Finnish Cancer Organizations, Sigrid Juselius Foundation and Gyllenberg Foundation.

Conflict of interest statement: IG received travel and research funding from Bristol-Myers Squibb (not related to this study); IR received honorarium, travel and research funding from Bristol-Myers Squibb (not related to this study). SM received honoraria and research funding from Bristol-Myers Squibb, Pfizer and Novartis (not related to this study). FG received honoraria from Novartis (not related to this study). SS received honoraria from Bristol-Myers Squibb, Incyte, Pfizer and Novartis and research funding from Bristol-Myers Squibb and Novartis (not related to this study). FXM is a consultant for Novartis and a speaker for Incyte biosciences, BMS, Novartis and Pfizer (not related to this study). The remaining authors declare no competing financial interests.

Significance (One sentence)
This mathematical modelling approach provides strong evidence that different immunological configurations in CML patients determine their response to therapy cessation and that dose reductions can help to prospectively infer different risk groups.

Abstract
Recent clinical findings in chronic myeloid leukemia (CML) patients suggest that the risk of molecular recurrence after stopping tyrosine kinase inhibitor (TKI) treatment substantially depends on an individual's leukemia-specific immune response. However, it is still not possible to prospectively identify patients that will remain in treatment-free remission (TFR). Here, we used an ordinary differential equation (ODE) model for CML, which explicitly includes an anti-leukemic immunological effect and applied it to 21 CML patients for whom *BCR-ABL1/ABL1* time courses had been quantified before *and* after TKI cessation. Immunological control was conceptually necessary to explain TFR as observed in about half of the patients. Fitting the model simulations to data, we identified patient-specific parameters and classified patients into three different groups according to their predicted immune system configuration ("immunological landscapes"). While one class of patients required complete CML eradication to achieve TFR, other patients were able to control residual leukemia levels after treatment cessation. Among them were a third class of patients, that maintained TFR only if an optimal balance between leukemia abundance and immunological activation was achieved before treatment cessation. Model simulations further suggested that changes in the *BCR-ABL1* dynamics resulting from TKI dose reduction convey information about the patient-specific immune system and allow prediction of outcome after treatment cessation. This inference of individual immunological configurations based on treatment alterations can also be applied to other cancer types in which the endogenous immune system supports maintenance therapy, long-term disease control or even cure.

Introduction

Chronic myeloid leukemia (CML) is a myeloproliferative disorder, which is characterized by the unregulated proliferation of immature myeloid cells in the bone marrow. CML is caused by a chromosomal translocation between chromosomes 9 and 22. The resulting BCR-ABL1 fusion protein acts as constitutively activated tyrosine kinase triggering a cascade of protein phosphorylation, which deregulate cell cycle, apoptosis regulation, cell adhesion and genetic stability. Due to their unregulated growth and their distorted differentiation, immature leukemic cells accumulate and impair normal hematopoiesis in the bone marrow, leading to the patient's death if left untreated.

Tyrosine kinase inhibitors (TKIs) specifically target the kinase activity of the BCR-ABL1 protein with high efficiency and have been established as the first line treatment for CML patients (1). Individual treatment responses are monitored by measuring the proportion of *BCR-ABL1* transcripts relative to a reference gene, e.g. *ABL1* or *GUS*, in blood cell samples by using Reverse Transcription and quantitative real-time polymerase chain reaction (RT-qPCR) (2–4). Most patients show a typical bi-exponential treatment response with a rapid, initial decline (α slope), followed by a moderate, second decline (β slope) (5–7). Whereas the initial decline can be attributed to the eradication of proliferating leukemic cells, the second decline has been suggested to result from a slower eradication of quiescent leukemic stem cells (3,4,8,9). Within five years of treatment, about two thirds of the patients achieve a major molecular remission (MMR), i.e. a *BCR-ABL1* reduction of three logs from the baseline (MR3), while at least one third of these additionally achieve a deep molecular remission (DMR, i.e. MR4 or lower) (4,7,10).

TKI discontinuation has been established as an experimental option for well responding patients with DMR for at least one year (11,12). Different studies independently confirmed that about half of the patients show a molecular recurrence, while the others stay in sustained treatment-free remission (TFR) after TKI stop. Consistently, most patients present with a recurrence within 6 months, while only a few cases are observed thereafter (11–14). The overall good response of those patients after restarting treatment with the previously administered TKI indicates that clonal transformation and resistance occurrence is not a primary problem in CML. As it appears unlikely that even a sustained remission truly indicates a complete eradication of the leukemic cells, other factors have to account for a continuing control of a minimal, potentially undetectable residual leukemic load. Although treatment discontinuation is highly desirable to reduce treatment-related side-effects and lower financial expenditures (15,16), it is still not possible to prospectively identify those patients that are at risk for a molecular recurrence. Investigations of clinical markers and scores to predict the recurrence behavior of patients after the treatment cessation revealed that both TKI treatment duration and the duration of a DMR were also associated with a higher probability of TFR (11,13,17,18). However, it is still unclear whether the dynamics of the initial TKI treatment response (e.g. the initial slope of decline) correlate with the remission occurrence after treatment discontinuation.

The underlying mechanisms of the recurrence behavior after TKI stop are still controversial. While fewer recurrences for patients with longer treatment suggest that a leukemic stem cell exhaustion is an important determinant, it is not a sufficient criteria to prospectively identify non-recurring patients (13,17). Favorable outcomes of treatment discontinuation for patients that were previously treated with immune-modulating drugs, such as IFN-α, suggest that immunological factors might play an additional and important role (11,18,19). In this context, it has been

demonstrated that specific subpopulations of dendritic cells and natural killer cells, as well as the cytokine secretion rate of natural killer cells are associated with higher probabilities of a treatment-free remission (20,21). Furthermore, there are several reports about patients with low but detectable *BCR-ABL1* levels over longer time periods after therapy discontinuation that do not relapse (14,22). This is a strong indicator that also other control mechanisms, such as the patient's immune response, are important determinants of a TFR.

Mathematical oncology has been established as a complementary effort to obtain insights into cancer biology and treatment. At the same time, model-based understanding of individual patient records is developing into a key method for devising adaptive therapies in the coming era of personalized medicine (23–26). CML is a show-case example, where several models have propelled the conceptual understanding of CML treatment dynamics (5–7,9,27–33) and are considered for the design of new clinical trials (34). Especially the long-term effect of TKI treatment on residual stem cell numbers and the effect of combination therapies were in focus. In a recent publication, we provided evidence that TKI dose reduction is a safe strategy for many patients in sustained remission while preserving the anti-leukemic effect (9). Complementary efforts also accounted for interactions between leukemic and immune cells (35–39). In a prominent approach, Clapp et al. used a CML-immune interaction to explain fluctuations of *BCR-ABL1* transcripts in TKI-treated CML patients (37). However, it remains elusive to which extend an immunological control is a crucial mediator to distinguish patients that maintain TFR from those that will eventually relapse.

Here, we used *BCR-ABL1* time courses of TKI-treated CML patients that were enrolled in previously published TKI discontinuation studies from different centers in Europe. In particular, we focused on patients for which *complete time courses* during the initial TKI therapy *and* after treatment cessation are available. Therefore, potential correlations between response dynamics, remission occurrences and timings after cessation become accessible. Motivated by the observation that the initial treatment response before TKI cessation does not show obvious correlations with remission occurrences, we aim to explain the resulting dynamics in terms of an ordinary differential equation (ODE) model of TKI-treated CML. Explicitly including a patient-specific, CML dependent immune component we are able to demonstrate that three different immunological configurations can determine the overall outcome after treatment cessation. We further investigate how this patient-specific configuration can be estimated from system perturbations, such as TKI dose reduction scenarios prior to treatment cessation. Our predictions closely resemble recent clinical findings substantiating our conclusion that treatment response during TKI dose reduction is indeed informative to predict a patient's future outcome after stopping therapy (40).

Methods

Patient selection

We analyzed time courses of 60 TKI-treated CML patients, for whom TKI-therapy had been stopped as a clinical intervention. Informed written consent was obtained from each subject according to the local regulations of the participating centers. Corresponding clinical trials were conducted in accordance with the Declaration of Helsinki and applicable regulatory requirements. The protocols were approved by the institutional review board or ethics committee of each participating center. Detailed information on the patient cohort is available in the Supplement Materials. For all 60 patients, serial *BCR-ABL1/ABL1* measurements before as well as after cessation are available. For the purpose of this analysis, the date of a molecular recurrence after cessation was defined as the first detected *BCR-ABL1/ABL1*-ratio above 0.1%, indicating a loss of MR3, or the re-initiation of TKI treatment, whatever was reported first.

Furthermore, we selected patients, which received TKI monotherapy before stopping, which have been monitored at a sufficient number of time points to estimate the initial and secondary slopes and which present with the typical bi-exponential response dynamic (Figure 1A, Supplementary Material). The 21 selected patients, fulfilling those criteria, were compared with the full patient cohort (n=60) and showed no obvious differences for the initial *BCR-ABL1* levels, treatment duration, recurrence behavior, follow up duration, recurrence times and used TKI, and are, therefore, considered to be representative examples (Figure S1). Moreover, the overall recurrence behavior of the selected patient cohort is comparable to larger clinical studies (11,14).

Mathematical model of TKI-treated CML

For our analysis, we apply an ODE model, which we proposed earlier in a methodological article qualitatively comparing a set of CML models with different functional interaction terms between leukemic cells and immune cells (39).

This model is sketched in Figure 1B and formally described by:

$$\frac{dX}{dt} = p_{YX} * Y - p_{XY} * X \tag{1}$$

$$\frac{dY}{dt} = p_{XY} * X - p_{YX} * Y + p_y \left(1 - \frac{Y}{K_Y}\right) * Y - m * Z * Y - TKI * Y \tag{2}$$

$$\frac{dZ}{dt} = r_z + Z * p_z * \frac{Y}{{K_z}^2 + Y^2} - a * Z \tag{3}$$

The model distinguishes between a population of quiescent leukemic cells (X) and a population of actively cycling leukemic cells (Y), which proliferate with the rate p_Y, whereas the growth is limited by a carrying capacity K_y. Leukemic cells can switch reversibly between the active and the quiescent state with transition rates p_{XY} and p_{YX}. Apoptosis is negligible for the quiescent population X and can be efficiently integrated in the proliferation term for the activated cells Y. TKI treatment is modelled by a kill rate TKI, which acts on proliferating cells Y, but does not affect quiescent cells X. Furthermore, we do not explicitly include resistance occurrence in the current model as it does not present a major challenge in CML treatment. A complete eradication of leukemic cells is defined as a decrease of leukemic cells in X and Y below the threshold of one cell. The corresponding *BCR-ABL1/ABL1* ratio in the peripheral blood are calculated as the ratio of proliferating leukemic cells to the carrying capacity K_Y (see Supplementary Material for details).
Furthermore, the model integrates a population of CML-specific immune effector cells (Z), which are generated at a constant, low production rate r_z and undergo apoptosis with rate a. They eliminate proliferating leukemic cells Y with the kill rate m. The leukemia-dependent recruitment of immune cells follows a nonlinear functional response where p_Z and K_Z are positive constants. This functional response leads to an *optimal* immune cell recruitment for intermediate leukemic cell levels, i.e.: for low numbers of proliferating leukemic cells ($Y < K_Z$), the immune cell recruitment increases and the immune cells Z are stimulated to replicate in presence of proliferating leukemic cells Y, reaching a maximum $p_Z/(2K_Z)$ when $Y = K_Z$. For higher leukemic cell numbers ($Y > K_Z$) the immune cell recruitment decreases with Y, reflecting the assumption that the proliferation of immune cells is decreased for high levels of proliferating leukemic cells Y. This assumption follows recent findings, suggesting that a high load of CML cells inhibits the immune effector cells' function and number (41). As a result, we obtain an *immune window* for which the recruitment exceeds the degradation rate a of the immune cells and leads to an optimal immune response (see Supplementary Material).

For all patients, we use fixed, universal values for the immune mediated killing rate m, the proliferation rate p_Y, the carrying capacity K_Y, the immune cells natural influx r_z and the immune cells apoptosis rate a. In contrast, the transition rates p_{XY} and p_{YX}, the TKI kill rate TKI and the immune parameters K_z and p_z are considered patient-specific parameters and are estimated with different strategies (see Supplementary Material).

Results

Individual *BCR-ABL1* dynamics after TKI stop can be explained by a patient-specific immune component

Comparing the *BCR-ABL1* kinetics of the 21 TKI-treated CML patients *before* treatment cessation, we detected no obvious differences between the recurring and non-recurring patient groups, i.e., we found no markers in the patient data which could potentially serve as a predictive measure to prospectively identify patients that show a treatment-free remission *after* treatment cessation (see Supplementary Material and Figure S2/3). Motivated by these results, we developed an ODE model of CML treatment to investigate which part of a patient's individual therapy response confers the relevant information to reliably distinguish recurrence from non-recurrence patients. To do so, we investigated which level of model complexity and what type of patient data are necessary as inputs to obtain model fits that sufficiently represent the available *BCR-ABL1* data before *and* after treatment stop and that would allow to anticipate the response dynamics to TKI cessation. The models and input data used in each fitting strategy are presented below, with an increasing level of complexity.

As a *reference* model, we use a reduced version of the suggested ODE model *without* an immunological component, i.e. all immunological parameters values are set to zero (Figure 1B; see Methods, $p_Z = K_Z = a = r_Z = m = 0$). This model predicts a complete eradication of residual disease levels only for very long treatment times. Thus, treatment cessation at any earlier time point will eventually lead to recurrence. Adapting this model to each available, individual patient time course by estimating the patient-specific model parameters p_{XY}, p_{YX} and TKI from the *pre-cessation BCR-ABL1* data, we confirm that relapse is predicted for all patients (Figure 2A, example time courses in Figures 2B,C), which is in contrast to the clinical observations. In summary, the reference model without immune system is not suitable to describe the non-recurrence cases and thereby opposes clinical findings on TFR (11–14).

Clinical studies suggest that immunological components can potentially control minimal residual disease levels and, therefore, might prevent (molecular) recurrences after TKI stop (20,21). Therefore, we use the ODE model (Methods, equations 1-3) that explicitly considers an immune component (39). Because measurements of individual anti-leukemic immune conditions are not available, we investigate three different approaches (fitting strategy I to III) for estimating the relevant immune parameters K_z and p_z and compare the corresponding simulation results with the clinical data.

In *fitting strategy I*, we consider a generic immune system configuration with *identical* immune parameters K_z and p_z for all patients. The remaining parameters p_{XY}, p_{YX} and TKI are estimated by individually fitting the model to the pre-cessation *BCR-ABL1* time courses. A grid-based search in the (K_z, p_z) space of immune parameters only identifies configurations in which the overall rates and timings of recurrence are not sufficiently met (Figure 2D). Furthermore, the model predictions fail on the individual level, as neither the time courses nor the recurrence behavior could be

predicted reliably (Figure 2D inset). These findings as well as the recognition of immunological differences between different patients argues in favor of patient-specific immune parameters.

In *fitting strategy II*, besides parameters p_{XY}, p_{YX} and TKI, we also estimate patient-specific values for immune parameter K_z and p_z; however we only apply the fitting routine to the *pre-cessation BCR-ABL1* time courses. We observe no statistically significant difference between recurring and non-recurring patients with respect to the fitted immune parameter values (Figure S4). Furthermore, the optimal fits fail to correctly predict the outcomes for individual patients (Figure 2E). This indicates that the configuration of the immune response is most likely not imprinted in the patient response under TKI treatment, in which the drug mediated leukemia reduction is the dominating process.

In *fitting strategy III*, we provide *pre- and post-cessation* data to fit patient specific model parameters p_{XY}, p_{YX}, TKI, K_z and p_z. We demonstrate that a *patient-specific* immune configuration is sufficient to consistently explain the clinical data (example time courses in Figure 2B,C, complete data in Figure S5 and Table S1), and that it can be obtained from patient's response after TKI stopping. The model correctly describes the behavior on the population level (Figure 2F), as well as on the individual patients (Figure 2F inset).

Having a univariate look at the individually estimated parameters of the immune model using fitting strategy III (Figure 3 A-E), we observed only minor differences between the recurring and the non-recurring patients, that do not allow to clearly distinguish the patient groups. However, a bivariate analysis of the immune parameters K_z and p_z reveals a distinction between recurrence and non-recurrence cases (Figure 3F). In particular, a lower value for the location of the immune window K_z together with a higher proliferation of the immune cells p_z convey a favorable outcome after therapy stop. This pattern is also confirmed at the level of individual patients in which we studied the predicted outcome for optimal fits with systematically varying immune parameters (Figure 3G and S6). This analysis reveals distinct parameter regions for which either remission or recurrence is predicted, although the precise location of those regions further depends on all model parameters.

From these results, we conclude that an individual immunological component (or another TKI-independent anti-leukemic effect) is necessary to quantitatively explain the individual *BCR-ABL1* time courses of CML patients before *and* after stopping the TKI treatment. Our results also suggest that the correct estimation of the parameters describing such immunological component for each patient is not possible based on the *BCR-ABL1* dynamics under constant TKI treatment alone and cannot be used for the prospective prediction of the molecular recurrence after TKI stop.

Individual recurrence classification based on an "immunological landscape"

Dynamical models, as the one suggested here for the interaction between leukemic and immunological cells (Figure 4A), are characterized by steady states which describe configurations in which the model quantities (in our case, cell populations) have reached an equilibrium. Stable steady states and their basins of attractions are conveniently depicted in a state space representation, which mimics a physical landscape (42) (Figure 4B). Typical steady states in our model refer to a fully developed leukemia ("disease steady state", $Y \approx K_Z$) or an immunological control of residual leukemic levels ("remission steady state", $Y \ll K_Z$), while trajectories represent dynamical changes of the system state along time. The existence and the precise location of the steady states and their basins of attraction depend on the particular leukemic and immunological model parameters and thereby determines the range of possible steady states that can be

achieved after treatment cessation (Figure 4C). As these parameters, obtained from fitting strategy III, differ between individual patients, they also describe “patient-specific immunological landscapes”.
A detailed mathematical analysis suggests that the available patients can be grouped in three general classes which correspond to structurally different underlying landscapes of the ODE model:

- Class A: For certain parameter configurations, the immunological landscape has only one stable steady state, namely the recurrence steady state E_H. This means that the patient will always present with recurring disease after treatment cessation in this model due to an *insufficient immune response,* if CML is not completely eradicated, irrespective of the degree of tumor load reduction. The corresponding immunological landscape is visualized in Figure 5A and depicts the recurrence behaviour depending on the number of immune cells and leukemic cells at treatment cessation. According to our estimates, 6 out of 21 patients fall into class A and ultimately present with recurring disease after treatment cessation (example in Figure 5B).
- Class B: For other parameter configurations, the immunological landscape has two stable steady states: the disease steady state E_H and the remission steady state E_L. In this case there is a distinct remission level of *BCR-ABL1* abundance, below which a *strong immune system* can further diminish the leukemia without TKI support. The corresponding immunological landscape is divided into these two basins of attraction and is visualized in Figure 5C. We estimate 8 out of 21 patients in this class, which all maintain TFR (example in Figure 5D).
- Class C: The third class has the same stable steady states as class B, but in this case a small disturbance from the cure steady state E_0 leads to the attraction basin of the recurrence steady state E_H instead of the remission steady state E_L. Only for a small range of CML abundance and a sufficiently high level of immune cells, the immune system is appropriately activated to keep the leukemia under sustained control. Figure 5E/F illustrates this control region as an isolated attractor basin. In the ideal case, the TKI therapy only reduces the leukemic load to a level that is sufficient to still activate the immune system to achieve this balance. However, if TKI treatment reduces tumor load to a very deep level, the CML cells regrow after therapy cessation as the immune response was also reduced too much. This represents a CML patient which may potentially achieve TFR but has a *weak immune response*. We estimate that seven out of 21 patients fall in this class, of which four have a recurrence and three remain in TFR (two examples in Figures 5G/H).

For completeness, there is a fourth class, in which only a cure steady state exists. In this case, CML would not develop at all due to a strongly suppressive immune system. Naturally, those individuals do not appear in the patient cohort at all.

Treatment optimization informed by the immunological configuration
We showed that the immunological configuration of each patient determines which steady states can be reached using TKI treatment. It should be pointed out, that the resulting conclusion does not depend only on the model fits to the data, but also on the particular mechanisms assumed by the model structure. Within those restrictions it appears that patients in class A can only stop TKI treatment in the case that the disease is completely eradicated. This would require a median treatment time of 29 years in our simulations and was not achieved in any of the considered patients. However, even if treatment cessation is not an option for these patients, our previously

published results suggests that TKI dose reduction could be considered as a long-term treatment alternative (9).

From a perspective of treatment optimization, patients in classes B and C are most interesting as they present an *immune window,* in which a TKI-based reduction of the leukemic cells can sufficiently stimulate the expansion of the immune cell population (Figure S7, Supplementary Material). Our model suggests that patients in class B are characterized by an immunological response that is sufficient to control the leukemia once the leukemic load has initially been reduced below a certain threshold. This remission allows for an activation of the immune system to further control the leukemia eradication even in the absence of TKI treatment. It is essential that the initial remission and the immunological activation surpass a certain threshold, which is indicated by the line separating the different basins of attraction in Figures 4B and 5C (separatrix). Clinically, this can be achieved by a sufficiently long TKI therapy, although we predict that this necessary time span was already reached much earlier for the respective six patients, in comparison with their actual treatment times (Table S2).

In contrast to class B, the model analysis implies that patients in class C can also present with recurrence if a long TKI treatment is applied. Only in a narrow region of CML abundance the immune system is sufficiently stimulated: if leukemic load is too high, the immunological component is still suppressed, while for too low levels the stimulation is not strong enough. In this respect, TFR can only be achieved if treatment keeps the patient within his individualized immune window for a sufficient time thereby supporting the adequate proliferation of immune cells, such that the patient reaches the basin of attraction of the remission steady state E_L (Figures 6A/B). If the treatment intensity is too high or the treatment duration is too long, this might lead to an "overtreatment" where the inherent immunological defense is not quickly and sufficiently activated to control a recurrence once TKI is stopped (Figures 6C-H). We show with a hypothetical treatment protocol that an adjustment of the necessary balance between leukemia abundance and immunological activation can be achieved within this model by detailed assessment of both cell populations and a narrowly adapted TKI administration (Figures S8/9).

TKI dose alteration informs molecular recurrence after treatment cessation

Detailed information about a patient's response to TKI treatment cessation (according to fitting strategy III) can only be obtained if the complete data (including post-cessation measurements) is available. Thus, this approach can obviously not serve as a prediction strategy *before* therapy stop. However, we show in the following that response to dose reduction – prior to therapy stop – will also provide information to identify the patient specific immunological landscape and is, therefore, likely to provide important information about the disease dynamics after treatment cessation. Both, clinical and modeling evidence support the strategy to use information from intermediate dose reduction as this appears as a safe treatment option for almost all well responding CML patients (9,43).

Specifically, individual fits for all patients according to the immune model and fitting strategy III allow to mathematically simulate how the patients would have responded if they were treated with a reduced TKI dose instead of stopping TKI completely. We use these model simulations to derive information about the predicted *BCR-ABL1* ratio during a 50% dose reduction within a 12-month period. Figure 7A/B illustrates two typical time courses.

Quantitatively, we estimate the linear slopes of the individual *BCR-ABL1/ABL1* response during dose reduction and correlate it to the final remission status after treatment cessation (Figure 7C). A logistic regression analysis reveals that a 0.01 increase in the estimated slope increases the

chance of recurrence by 21% (OR: 1.21, 95% CI: 1.07–1.51), thereby indicating that recurring patients are predicted to present with higher (positive) slopes of the *BCR-ABL1* ratio during the dose reduction period. Moreover, complementing this plot with the association of each patient with its predicted particular response class A, B, or C, we observe that class A patients have higher positive slopes and always have a recurrence, while most of class B patients show constant *BCR-ABL1* levels, therefore, staying in TFR. Class C patients show both, constant or increasing *BCR-ABL1* levels. However, higher positive slopes are more often observed in recurring patients. We suggest that patients with pronounced increases in *BCR-ABL1* levels after dose reduction should not stop TKI treatment as this increase points towards an insufficient immune control and conveys an increased risk for molecular recurrence.

Our results are in qualitative and quantitative agreement with a recent reanalysis of clinical data from the DESTINY trial (NCT01804985)(43,44) which differs from other TKI stop studies as in this trial the TKI treatment is reduced to 50% of the standard dose for 12 months prior to cessation. Based on a dataset of 171 patients we could demonstrate that the patient-individual slope of *BCR-ABL1/ABL1* ratios monitored during TKI dose reduction strongly correlates with the risk of individual recurrence after TKI stop (OR: 1.28; 95% CI: 1.17-1.42) and can serve as a promising indicator for high risk patients (40). Although time courses prior to dose reduction are not available from this study and preclude fitting of the complete ODE model, the overall conclusion of both, the presented conceptual approach and a paralleling data analysis, suggest that dose alterations are a valid means to probe the immunological configuration of leukemic remission.

Discussion

Here we present an ODE model for CML treatment that explicitly includes an immunological component and apply it to describe the therapy response and recurrence behavior of a cohort of 21 CML patients with detailed *BCR-ABL1* follow-up over their whole patient history. We demonstrate that an anti-leukemic immunological mechanism is necessary to account for a TKI-independent disease control, which prevents molecular recurrence emerging from residual leukemic cell levels after TKI cessation. Without such a mechanism, a long-term TFR can only be achieved if a complete eradication of leukemic cells is assumed. However, the presence of detectable MRD levels in many patients after therapy cessation (14) is not consistent with this assumption, which strongly suggests an additional control instance, which others (20,21,45,46) and we (39) interpret as a set of immunological factors. Including these aspects into our modeling approach, the available clinical data can be sufficiently described on the level of individual patients.

Based on our simulation results we classify patients into three different groups regarding their predicted immune system configuration (“immunological landscape”): *insufficient immune response* (class A), *strong immune response* (class B) and *weak immune response* (class C). Class A patients are not able to control residual leukemic cells and would always present with CML recurrence as long as the disease is not completely eradicated. Consistent with the results of Horn et al. (47), this is only accomplished on very long timescales in our simulations and would, therefore, result in a lifelong therapy for most affected patients. However, as we suggested earlier, those patients might be eligible for substantial TKI dose reductions during long-term maintenance therapy (9). In contrast, class B patients are predicted to have a strong immune response and to control the leukemia once the leukemic load has been reduced below a certain threshold and thus, are predicted to require only a minimal treatment time (less than 5 years for the studied patients, see Table S2) to achieve TFR. For class C patients with a weak immune response, our model predicts that TFR achievement depends on an optimal balance between leukemia abundance and immunological activation before treatment cessation and could be accomplished by a narrowly

adapted TKI administration. These results are in line with those from a recent modeling study which suggested the existence a 'Goldilocks Window' in which treatment is required to optimize the balance between maximal tumor reduction and preservation of patient immune function (26).
We also show that the information required to classify the patients according to their immune response and to predict their recurrence behavior cannot be obtained from *BCR-ABL1* measurements *before* treatment cessation only. A different fitting strategy (III) assessing also *BCR-ABL1* measurements after treatment cessation shows that the *BCR-ABL1* changes resulting from this system perturbation (i.e. TKI stop) yields the necessary information. Interestingly, our simulation results demonstrate that also a less drastic system perturbation, i.e. a TKI dose reduction, can provide similar information and can be used to predict the individual outcome after treatment cessation. The feasibility of such an approach has been complemented by a recent reanalysis of the DESTINY trial (NCT01804985), which evaluated a beneficial effect of a 12 months dose reduction treatment prior to TKI stop. We could confirm based on the clinical data of 171 patients that the patient's response dynamic during TKI dose reduction is indeed predictive for the individual risk of CML recurrence after TKI stop (40,43).

Direct measurements of the individual immune compartments and their activation states represent another road to better understand the configuration of the anti-leukemic immune response in CML patients. Several studies identified different immunological markers in CML patients that correlate with the probability of treatment-free remission after therapy cessation (20,21). Learning from the behavior of these populations under continuing TKI treatment and with lowered leukemic load could further contribute to identify a patient's "immunological landscape" and be informative for the prediction of individual outcomes after treatment stopping. However, as it is not clear, which immunological subset provides the suggested observed anti-CML response (48,49), corresponding measurements are currently not feasible and strongly argue in favor of our indirect modeling approach suggesting to retrieve similar information from *BCR-ABL1* dynamics after TKI dose reduction.

Our analysis is based on a rather small cohort of patients. Although our results do not depend on the study size, we can derive the strongest conclusions with respect to illustrating the conceptual approach of inferring immune responses from treatment alterations and demonstrating its predictive power. Our results are further based on a set of simplifications and assumptions. As such, we do not consider resistance mutations as almost no such events have been reported during TKI cessation studies in CML and almost all patients respond well to re-initiation of TKI treatment with their previous drug (11). This might be different for other disease entities in which tumor evolution imposes serious challenges to long-term disease control. Focusing on a related aspect it has been shown that different immune cell types are associated with recurrence behavior of CML patients (20,21). However, for simplicity, we restricted our analysis to a unified anti-leukemic immune compartment in the model and did not distinguish between different immune cell populations and interactions between them. Furthermore, the model is based on an interaction between leukemic and immune cells, in which the immune cell population is only activated for intermediate levels of leukemic burden, reflecting the assumption that immune cells are not efficiently activated for small numbers of leukemic cells and are additionally suppressed by high tumor load. Similar assumptions have been discussed recently (37) while we also illustrated the suitability of other mechanisms of interaction (39).

In summary, our results support the notion of immunological mechanisms as an important factor to determine the success of TFR in CML patients. Importantly, we show that besides the direct measurement of the immune response, also system perturbations, such as a TKI dose reduction,

can (indirectly) provide information about the individual disease dynamics and, therefore, allow to predict the risk of CML recurrence for individual patients after TKI stop. Such results demonstrate the potential of mathematical models in providing insights on the mechanisms underlying cancer treatment as well in delineating different treatment strategies. Applications to other cancer entities, in which the endogenous immune system can support the control or even the eradication of residual tumor cells, are a natural continuation of this work and will become even more important with the availability of cancer immunotherapies that allow modulation of individual immune responses (50).

Acknowledgement
We thank all patients and hospital staff for providing this valuable data for scientific assessment.

References

1. Hochhaus A, Saussele S, Rosti G, Mahon F-X, Janssen JJWM, Hjorth-Hansen H, et al. Chronic myeloid leukaemia: ESMO Clinical Practice Guidelines for diagnosis, treatment and follow-up. Annals of Oncology. 2017;28:iv41–51.

2. Pasic I, Lipton JH. Current approach to the treatment of chronic myeloid leukaemia. Leukemia Research. 2017;55:65–78.

3. Rosti G, Castagnetti F, Gugliotta G, Baccarani M. Tyrosine kinase inhibitors in chronic myeloid leukaemia: which, when, for whom? Nature Reviews Clinical Oncology. 2017;14:141–54.

4. Apperley JF. Chronic myeloid leukaemia. The Lancet. 2015;385:1447–59.

5. Michor F, Hughes TP, Iwasa Y, Branford S, Shah NP, Sawyers CL, et al. Dynamics of chronic myeloid leukaemia. Nature. 2005;435:1267–70.

6. Roeder I, Horn M, Glauche I, Hochhaus A, Mueller MC, Loeffler M. Dynamic modeling of imatinib-treated chronic myeloid leukemia: functional insights and clinical implications. Nature Medicine. 2006;12:1181–4.

7. Stein AM, Bottino D, Modur V, Branford S, Kaeda J, Goldman JM, et al. BCR-ABL Transcript Dynamics Support the Hypothesis That Leukemic Stem Cells Are Reduced during Imatinib Treatment. Clinical Cancer Research. 2011;17:6812–21.

8. Tang M, Gonen M, Quintas-Cardama A, Cortes J, Kantarjian H, Field C, et al. Dynamics of chronic myeloid leukemia response to long-term targeted therapy reveal treatment effects on leukemic stem cells. Blood. 2011;118:1622–31.

9. Fassoni AC, Baldow C, Roeder I, Glauche I. Reduced tyrosine kinase inhibitor dose is predicted to be as effective as standard dose in chronic myeloid leukemia: a simulation study based on phase III trial data. Haematologica. 2018;103:1825–34.

10. Cortes JE, Saglio G, Kantarjian HM, Baccarani M, Mayer J, Boqué C, et al. Final 5-Year Study Results of DASISION: The Dasatinib Versus Imatinib Study in Treatment-Naïve Chronic Myeloid Leukemia Patients Trial. Journal of Clinical Oncology. 2016;34:2333–40.

11. Saussele S, Richter J, Guilhot J, Gruber FX, Hjorth-Hansen H, Almeida A, et al. Discontinuation of tyrosine kinase inhibitor therapy in chronic myeloid leukaemia (EURO-SKI): a prespecified interim analysis of a prospective, multicentre, non-randomised, trial. The Lancet Oncology. 2018;19:747–57.

12. Okada M, Imagawa J, Tanaka H, Nakamae H, Hino M, Murai K, et al. Final 3-year Results of the Dasatinib Discontinuation Trial in Patients With Chronic Myeloid Leukemia Who Received Dasatinib as a Second-line Treatment. Clinical Lymphoma Myeloma and Leukemia. 2018;18:353-360.e1.

13. Mahon F-X, Réa D, Guilhot J, Guilhot F, Huguet F, Nicolini F, et al. Discontinuation of imatinib in patients with chronic myeloid leukaemia who have maintained complete molecular remission for at least 2 years: the prospective, multicentre Stop Imatinib (STIM) trial. The Lancet Oncology. 2010;11:1029–35.

14. Rousselot P, Charbonnier A, Cony-Makhoul P, Agape P, Nicolini FE, Varet B, et al. Loss of Major Molecular Response As a Trigger for Restarting Tyrosine Kinase Inhibitor Therapy in Patients With Chronic-Phase Chronic Myelogenous Leukemia Who Have Stopped Imatinib After Durable Undetectable Disease. Journal of Clinical Oncology. 2014;32:424–30.

15. Caldemeyer L, Dugan M, Edwards J, Akard L. Long-Term Side Effects of Tyrosine Kinase Inhibitors in Chronic Myeloid Leukemia. Current Hematologic Malignancy Reports. 2016;11:71–9.

16. Experts in Chronic Myeloid Leukemia. The price of drugs for chronic myeloid leukemia (CML) is a reflection of the unsustainable prices of cancer drugs: from the perspective of a large group of CML experts. Blood. 2013;121:4439–42.

17. Saussele S, Richter J, Hochhaus A, Mahon F-X. The concept of treatment-free remission in chronic myeloid leukemia. Leukemia. 2016;30:1638–47.

18. Takahashi N, Kyo T, Maeda Y, Sugihara T, Usuki K, Kawaguchi T, et al. Discontinuation of imatinib in Japanese patients with chronic myeloid leukemia. Haematologica. 2012;97:903–6.

19. Ross DM, Branford S, Seymour JF, Schwarer AP, Arthur C, Yeung DT, et al. Safety and efficacy of imatinib cessation for CML patients with stable undetectable minimal residual disease: results from the TWISTER study. Blood. 2013;122:515–22.

20. Schütz C, Inselmann S, Sausslele S, Dietz CT, Müller MC, Eigendorff E, et al. Expression of the CTLA-4 ligand CD86 on plasmacytoid dendritic cells (pDC) predicts risk of disease recurrence after treatment discontinuation in CML. Leukemia. 2017;31:829–36.

21. Ilander M, Olsson-Strömberg U, Schlums H, Guilhot J, Brück O, Lähteenmäki H, et al. Increased proportion of mature NK cells is associated with successful imatinib discontinuation in chronic myeloid leukemia. Leukemia. 2017;31:1108–16.

22. Mahon F-X. Treatment-free remission in CML: who, how, and why? Hematology Am Soc Hematol Educ Program. 2017;2017:102–9.

23. Altrock PM, Liu LL, Michor F. The mathematics of cancer: integrating quantitative models. Nature Reviews Cancer. 2015;15:730–45.

24. West JB, Dinh MN, Brown JS, Zhang J, Anderson AR, Gatenby RA. Multidrug Cancer Therapy in Metastatic Castrate-Resistant Prostate Cancer: An Evolution-Based Strategy. Clin Cancer Res. 2019;25:4413–21.

25. Brady R, Enderling H. Mathematical Models of Cancer: When to Predict Novel Therapies, and When Not to. Bull Math Biol. 2019;81:3722–31.

26. Park DS, Robertson-Tessi M, Maini P, Bonsall MB, Gatenby RA, Anderson AR. The Goldilocks Window of Personalized Chemotherapy: An Immune Perspective [Internet]. Cancer Biology; 2018 Dec. Available from: http://biorxiv.org/lookup/doi/10.1101/495184

27. Komarova NL, Wodarz D. Effect of Cellular Quiescence on the Success of Targeted CML Therapy. Agur Z, editor. PLoS ONE. 2007;2:e990.

28. Komarova NL, Wodarz D. Combination Therapies against Chronic Myeloid Leukemia: Short-term versus Long-term Strategies. Cancer Research. 2009;69:4904–10.

29. Glauche I, Moore K, Thielecke L, Horn K, Loeffler M, Roeder I. Stem cell proliferation and quiescence--two sides of the same coin. PLoS Comput Biol. 2009;5:e1000447.

30. Glauche I, Horn K, Horn M, Thielecke L, Essers MA, Trumpp A, et al. Therapy of chronic myeloid leukaemia can benefit from the activation of stem cells: simulation studies of different treatment combinations. British Journal of Cancer. 2012;106:1742–52.

31. Woywod C, Gruber FX, Engh RA, Flå T. Dynamical models of mutated chronic myelogenous leukemia cells for a post-imatinib treatment scenario: Response to dasatinib or nilotinib therapy. Komarova NL, editor. PLOS ONE. 2017;12:e0179700.

32. Nanda S, Moore H, Lenhart S. Optimal control of treatment in a mathematical model of chronic myelogenous leukemia. Mathematical Biosciences. 2007;210:143–56.

33. Krishchenko AP, Starkov KE. On the global dynamics of a chronic myelogenous leukemia model. Communications in Nonlinear Science and Numerical Simulation. 2016;33:174–83.

34. Schiffer JT, Schiffer CA. To what extent can mathematical modeling inform the design of clinical trials? The example of safe dose reduction of tyrosine kinase inhibitors in responding patients with chronic myeloid leukemia. Haematologica. 2018;103:1756–7.

35. Kim PS, Lee PP, Levy D. Dynamics and Potential Impact of the Immune Response to Chronic Myelogenous Leukemia. De Boer RJ, editor. PLoS Computational Biology. 2008;4:e1000095.

36. Wodarz D. Heterogeneity in chronic myeloid leukaemia dynamics during imatinib treatment: role of immune responses. Proceedings of the Royal Society B: Biological Sciences. 2010;277:1875–80.

37. Clapp GD, Lepoutre T, El Cheikh R, Bernard S, Ruby J, Labussiere-Wallet H, et al. Implication of the Autologous Immune System in BCR-ABL Transcript Variations in Chronic Myelogenous Leukemia Patients Treated with Imatinib. Cancer Research. 2015;75:4053–62.

38. Besse A, Clapp GD, Bernard S, Nicolini FE, Levy D, Lepoutre T. Stability Analysis of a Model of Interaction Between the Immune System and Cancer Cells in Chronic Myelogenous Leukemia. Bulletin of Mathematical Biology. 2018;80:1084–110.

39. Fassoni A, Roeder I, Glauche I. To Cure or Not to Cure: Consequences of Immunological Interactions in CML Treatment. Bull Math Biol [Internet]. 2019 [cited 2019 May 12]; Available from: http://link.springer.com/10.1007/s11538-019-00608-x

40. Gottschalk A, Glauche I, Cicconi S, Clark R, Roeder I. Molecular dynamics during reduction of TKI dose reliably identify molecular recurrence after treatment cessation in CML. Accepted for publication in Blood. 2019.

41. Hughes A, Clarson J, Tang C, Vidovic L, White DL, Hughes TP, et al. CML patients with deep molecular responses to TKI have restored immune effectors and decreased PD-1 and immune suppressors. Blood. 2017;129:1166–76.

42. Fassoni AC, Yang HM. An ecological resilience perspective on cancer: Insights from a toy model. Ecological Complexity. 2017;30:34–46.

43. Clark RE, Polydoros F, Apperley JF, Milojkovic D, Rothwell K, Pocock C, et al. De-escalation of tyrosine kinase inhibitor therapy before complete treatment discontinuation in patients with chronic myeloid leukaemia (DESTINY): a non-randomised, phase 2 trial. The Lancet Haematology. 2019;6:e375–83.

44. Clark RE, Polydoros F, Apperley JF, Milojkovic D, Pocock C, Smith G, et al. De-escalation of tyrosine kinase inhibitor dose in patients with chronic myeloid leukaemia with stable major molecular response (DESTINY): an interim analysis of a non-randomised, phase 2 trial. The Lancet Haematology. 2017;4:e310–6.

45. Rea D, Henry G, Khaznadar Z, Etienne G, Guilhot F, Nicolini F, et al. Natural killer-cell counts are associated with molecular relapse-free survival after imatinib discontinuation in chronic myeloid leukemia: the IMMUNOSTIM study. Haematologica. 2017;102:1368–77.

46. Hughes A, Yong ASM. Immune Effector Recovery in Chronic Myeloid Leukemia and Treatment-Free Remission. Frontiers in Immunology [Internet]. 2017 [cited 2018 Aug 6];8. Available from: http://journal.frontiersin.org/article/10.3389/fimmu.2017.00469/full

47. Horn M, Glauche I, Muller MC, Hehlmann R, Hochhaus A, Loeffler M, et al. Model-based decision rules reduce the risk of molecular relapse after cessation of tyrosine kinase inhibitor therapy in chronic myeloid leukemia. Blood. 2013;121:378–84.

48. Ilander M, Mustjoki S. Immune control in chronic myeloid leukemia. Oncotarget [Internet]. 2017 [cited 2019 Mar 6];8. Available from: http://www.oncotarget.com/fulltext/22279

49. Brück O, Blom S, Dufva O, Turkki R, Chheda H, Ribeiro A, et al. Immune cell contexture in the bone marrow tumor microenvironment impacts therapy response in CML. Leukemia. 2018;32:1643–56.

50. Zhang H, Chen J. Current status and future directions of cancer immunotherapy. J Cancer. 2018;9:1773–81.

Figure 1: Strategy for patient selection and model sketch of TKI-treated CML
(A) Flow diagram indicating the process of data selection. Patients were excluded with less than 5 *BCR-ABL1* measurements during TKI treatment, missing or extremely low initial measurements (i.e., first measurement is only available after more than 10 months or below MMR). Furthermore, we only included patients with a biexponential decline in which the initial slope was steeper than the second slope. We also selected patients that were under continuous therapy with one TKI, thereby excluding patients with a pre-treatment, TKI-change during, combination therapy and missing therapy/cessation information. **(B)** General scheme of the ODE model setup indicating the relevant cell populations and their mutual interactions (arrows with rate constants) that govern their dynamical responses. Leukemic cells can reversibly switch between the quiescent (X) and proliferating (Y) state with corresponding transition rates p_{XY} and p_{YX}. Proliferating cells divide with rate $p_y\left(1-\frac{Y}{K_Y}\right)$. The TKI treatment has a cytotoxic effect TKI on proliferating cells (thunder symbol) while quiescent cells are not affected. Immune cells in Z have a cytotoxic effect (with rate m) on proliferating leukemic cells in Y. The proliferation of immune cells is stimulated in the presence of proliferating leukemic cells by an immune recruitment rate $p_z * \frac{Y}{{K_z}^2+Y^2}$. This nonlinear term describes an immune window, where the immune response is suppressed for high leukemic cell levels above the constant K_z. Moreover, immune cells are generated by a constant production r_z and undergo apoptosis with rate a (see Methods).

Figure 2: Model comparison using different fitting strategies.
(A,D,E,F): Kaplan-Meier estimators comparing the cumulative recurrence rates of four different fitting strategies (grey) with the clinical data (black): (A) the reduced model *without* an immune component, and three different configurations of the immune model ((D): generic immune system configuration (fitting strategy I), (E): individual immune system configuration estimated by fitting pre-cessation data of the *BCR-ABL/ABL1* time courses (fitting strategy II); (F): individual immune system configuration estimated by fitting the complete *BCR-ABL/ABL1* time courses (fitting strategy III)). The insets show the rate of true positive (tp) and true negative (tn) predictions of the model. (**B, C):** Examples of clinical data for a representative recurring (B) and a non-recurring (C) patient with corresponding model predictions for the reduced model *without* an immune component (black) and the full model using an individual immune system configuration estimated by fitting complete *BCR-ABL/ABL1* time courses (fitting strategy III - grey). *BCR-ABL/ABL1* measurements are shown as black dots. Black triangles indicate the lower quantification limit for undetectable *BCR-ABL1* levels (see Supplementary Material). The grey area indicates the time period after treatment cessation.

Figure 3: Comparison of estimated immune model parameters for recurring and non-recurring patients.
(A-E) Violin plots of the best fit values for model parameters p_z, K_z, p_{XY}, p_{YX} and TKI obtained by using fitting strategy III, shown separately for the groups of recurring (dark grey) and non-recurring (light grey) patients. The individual parameter values are shown as short horizontal black (recurring patients) and white tick marks (non-recurring patients). The horizontal black lines indicate the median value of each group while the dashed grey line depicts the mean value of the complete cohort, P-values are based on a Kolmogorov-Smirnov tests to compare the distribution of the estimated parameters. (**F**): Scatter plot for the best fitting immune parameter p_z vs. K_z obtained for each patient (fitting strategy III) from the recurrence (dark grey) and non-recurrence group (light grey). **(G**) Predicted recurrence behavior (recurrence - dark grey; non-recurrence - light grey) for an individual patient depending on the values of the immune parameters (p_z, K_z) which are varied within a predefined grid. The remaining free parameters (p_{XY}, p_{YX}, TKI) were optimized according to fitting strategy III. Only parameter estimations resulting in sufficiently good fits (i.e. with a residual sum of squares (RSS) less than twice the RSS of the best fit) are shown. Figure S6 provides the corresponding plots for all 21 patients.

Figure 4: Conceptual approach to obtain immunological landscapes.
(A) A set of optimal, patient specific model parameters is obtained by fitting the ODE model to the pre- and post-cessation *BCR-ABL1* time courses of each patient (black lines indicating the optimal model fit to the data). (**B)** Based on the obtained parameters, a phase portrait of system (equations 1-3) can be reconstructed, in which the abundance of leukemic (in terms of *BCR-ABL/ABL1* ratio) and immune cells are shown on the respective axes. For the situation of no TKI treatment (TKI=0), several stable steady states can be identified to which the system would converge in the long run. Typically, the *disease steady state* E_H is characterized by a high number of leukemic cells and few immune cells while in the *remission steady state* E_L an increased number of immune cells exerts control of a residual leukemic disease. Each stable steady state has a basin of attraction, which is the set of all points that approach the stable point as time passes. A completely eradication of leukemic cells constitutes the *cure steady state* E_0, which is intrinsically unstable and does not have a basin of attraction. At diagnosis, the system state is near the disease steady state and will remain there unless the TKI treatment drives the system away from this basin of attraction (green trajectory, lowering the abundance of leukemic cells). The outcome after treatment cessation depends on whether the trajectory has crossed the separatrix (dashed line separating the different basins of attraction) or not (indicated by the orange or purple star, respectively). The system either returns to the disease steady state indicating recurrence (red trajectory) or approaches the remission steady state (blue trajectory), indicating sufficient immune activation and sustained disease control. The resulting “immunological landscape” is patient specific and the location of the separatrix may differ for different patients. This implies that the minimum level of leukemic cells to guarantee TFR differs between patients. **(C)** Given the particular model parameterization and the resulting immunological landscape for each patient, it is now possible to simulate different treatment scenarios for that particular patient including different cessation times (indicated by the orange or purple star).

Figure 5: Immunological landscapes for typical clinical scenarios and corresponding time courses.

(A,C,E,G) Examples of patient specific landscapes are shown on the left side (compare Figure 4). The disease and remission state are represented by solid circles (●). The y-axis (BCR-ABL/ABL) is set to a nonlinear scale via a root transformation. The black solid line describe trajectories under TKI treatment, while the grey line describes the time course after treatment cessation. **(B,D,F,H)** Corresponding clinical data (dots and triangles, compare Figure 2B,C) and optimal simulation results (black line – predicted *BCR-ABL/ABL1* ratio, grey line – predicted number of immune cells) are shown on the right side (compare Figure 2B,C). Horizontal dashed lines indicate the immune window if it exists (c.f. Methods, Supplementary Material). **(A,B)** For patients in class A (insufficient immune response), only the disease steady state E_H is available, and all trajectories lead to recurrence after treatment cessation. **(C,D)** Class B patients (strong immune response) present with the disease steady state E_H and remission steady state E_L. The separatrix between their basins of attraction is represented by a dashed line. After treatment cessation, the patients stays in TFR. (**E-H)** Patients of class C (weak immune response) present with an isolated basin of attraction for the remission steady state E_L which is more difficult to reach. The example in (E,G) maintains TFR after TKI cessation while the lower example in (F,H) presents with recurrence.

Figure 6: Predicted recurrence behavior of patients with weak immune response (class C).

Typical immunological landscapes, as they can occur for patients with a weak immune response (class C), are complemented with corresponding simulation time courses for *BCR-ABL/ABL1* ratio and immune cell number for different simulated treatment times (c.f. Figure 5). **(A,B)** TKI treatment "drives" the system within the isolated basin of the remission steady state E_L, and the simulated patient achieves TFR. **(C,D)** Using the same parameterization as in (A,B) but a longer treatment time makes the trajectory leave the basin of attraction for the remission steady state. This leads to a considerable decrease in the recruitment of immune cells and results in recurrence after TKI cessation. **(E,F,G,H)** For another parameterization of the ODE model, the treatment trajectory would never reach the basin of the remission steady state, independent of the applied treatment time (35 months in E,F; 70 months in G,H), and ultimately lead to disease recurrence.

Figure 7: Simulation of individual responses to TKI dose reduction and association with the final remission state

(A,B) Representative time courses illustrate simulated patient responses (in terms of *BCR-ABL/ABL1* ratios (black line) and number of immune cells (grey line), compare Figure 5) under the assumption that the TKI dose is reduced to 50% of the initial dose during a 12 month dose reduction period (grey background). From these simulations, the linear slope of the log(BCR-ABL/ABL) ratio during the dose reduction period (dashed white line, the inset shows an enlarged view of the dose reduction period) is obtained using a linear regression model.

(C) Logistic regression analysis for the remission status of all 21 patients after treatment cessation (either recurring or non-recurring; class indicated by symbol: class A: circle, class B: square, class C: rhombus, overlapping points are stacked horizontally (*)) versus their simulated log(BCR-ABL/ABL) slope during the 12 month dose reduction period. The solid line indicates the estimated chance that a patient presenting with the particular slope during dose reduction will show disease recurrence after finally stopping TKI treatment. The corresponding OR = 1.21 (95% CI: 1.07–1.51) indicates that the chance for disease recurrence after TKI stop increases by 21% for each 0.01 increase in the log10(BCR-ABL/ABL) slope during dose reduction.

Figure 1

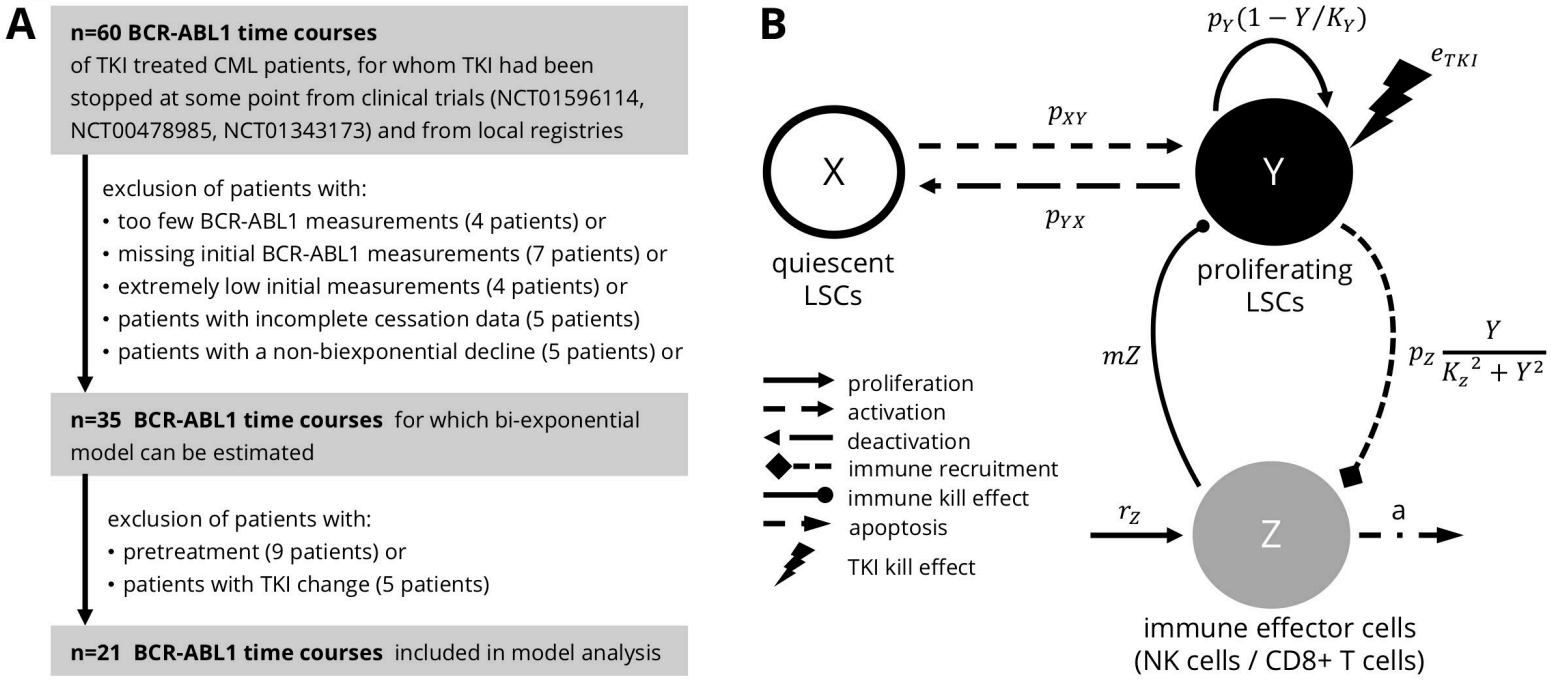
A
n=60 BCR-ABL1 time courses
of TKI treated CML patients, for whom TKI had been stopped at some point from clinical trials (NCT01596114, NCT00478985, NCT01343173) and from local registries
exclusion of patients with:
• too few BCR-ABL1 measurements (4 patients) or
• missing initial BCR-ABL1 measurements (7 patients) or
• extremely low initial measurements (4 patients) or
• patients with incomplete cessation data (5 patients)
• patients with a non-biexponential decline (5 patients) or
n=35 BCR-ABL1 time courses for which bi-exponential model can be estimated
exclusion of patients with:
• pretreatment (9 patients) or
• patients with TKI change (5 patients)
n=21 BCR-ABL1 time courses included in model analysis
B
$p_Y(1 - Y/K_Y)$
e_{TKI}
p_{XY}
p_{YX}
X
Y
quiescent LSCs
proliferating LSCs
mZ
$p_Z \frac{Y}{K_z{}^2 + Y^2}$
proliferation
activation
deactivation
immune recruitment
immune kill effect
apoptosis
TKI kill effect
r_Z
Z
a
immune effector cells
(NK cells / CD8+ T cells)

Figure 2

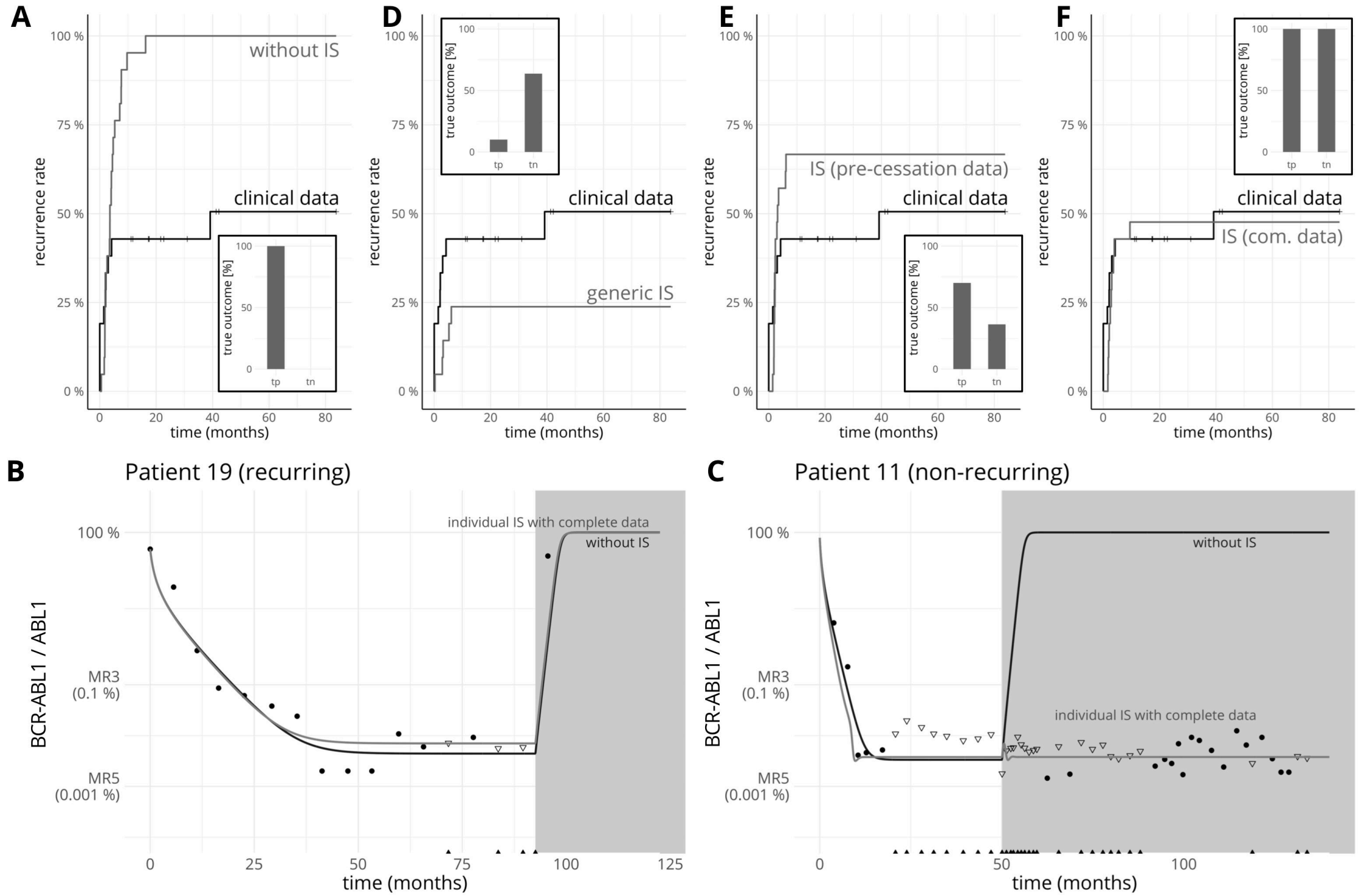
A
without IS
clinical data
recurrence rate
time (months)
true outcome [%]
tp
tn
D
clinical data
generic IS
E
IS (pre-cessation data)
clinical data
F
clinical data
IS (com. data)
B
Patient 19 (recurring)
individual IS with complete data
without IS
BCR-ABL1 / ABL1
MR3
(0.1 %)
MR5
(0.001 %)
C
Patient 11 (non-recurring)
without IS
individual IS with complete data

Figure 3

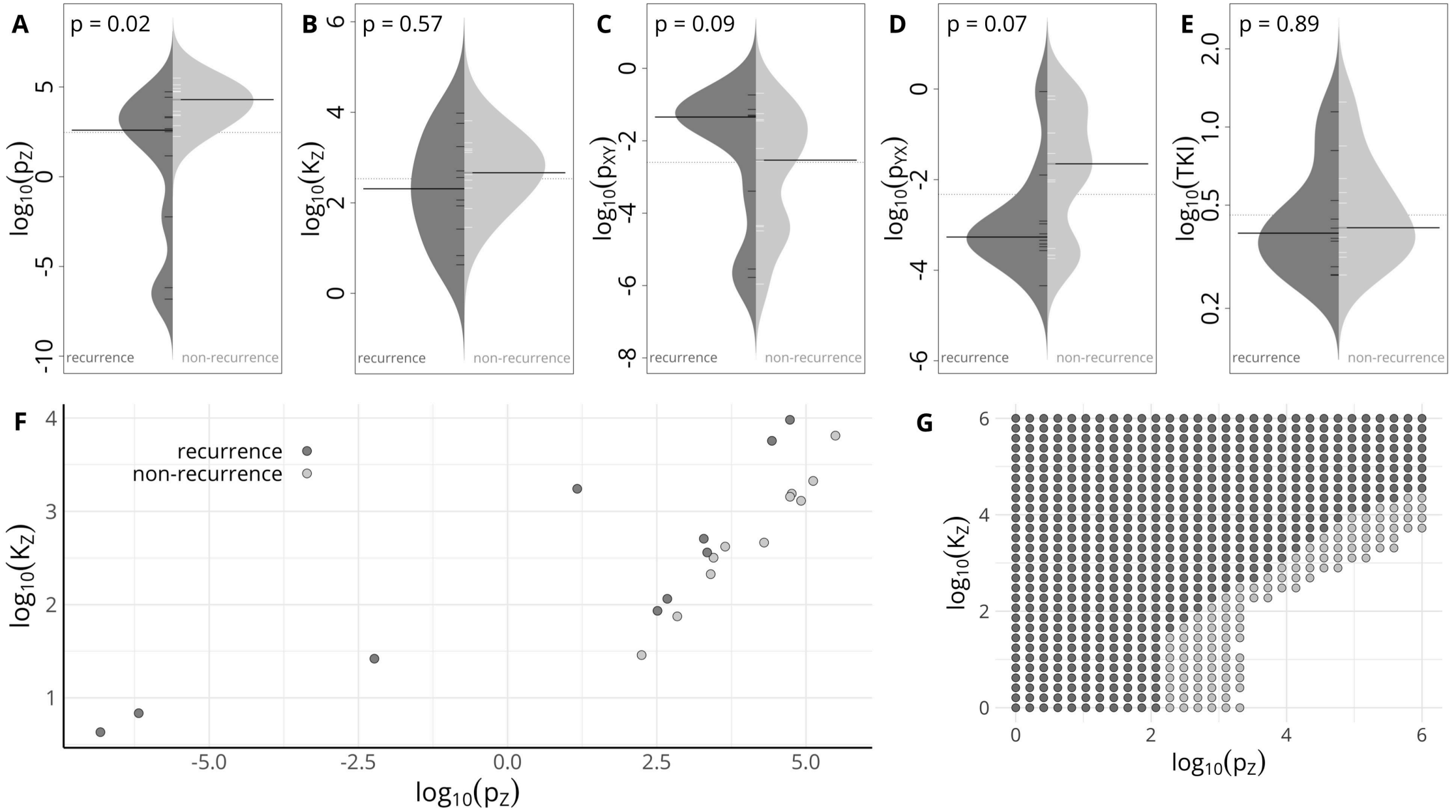
A
p = 0.02
log10(pZ)
recurrence
non-recurrence
B
p = 0.57
log10(KZ)
C
p = 0.09
log10(pXY)
D
p = 0.07
log10(pYX)
E
p = 0.89
log10(TKI)
F
recurrence
non-recurrence
log10(KZ)
log10(pZ)
G
log10(KZ)
log10(pZ)

Figure 4

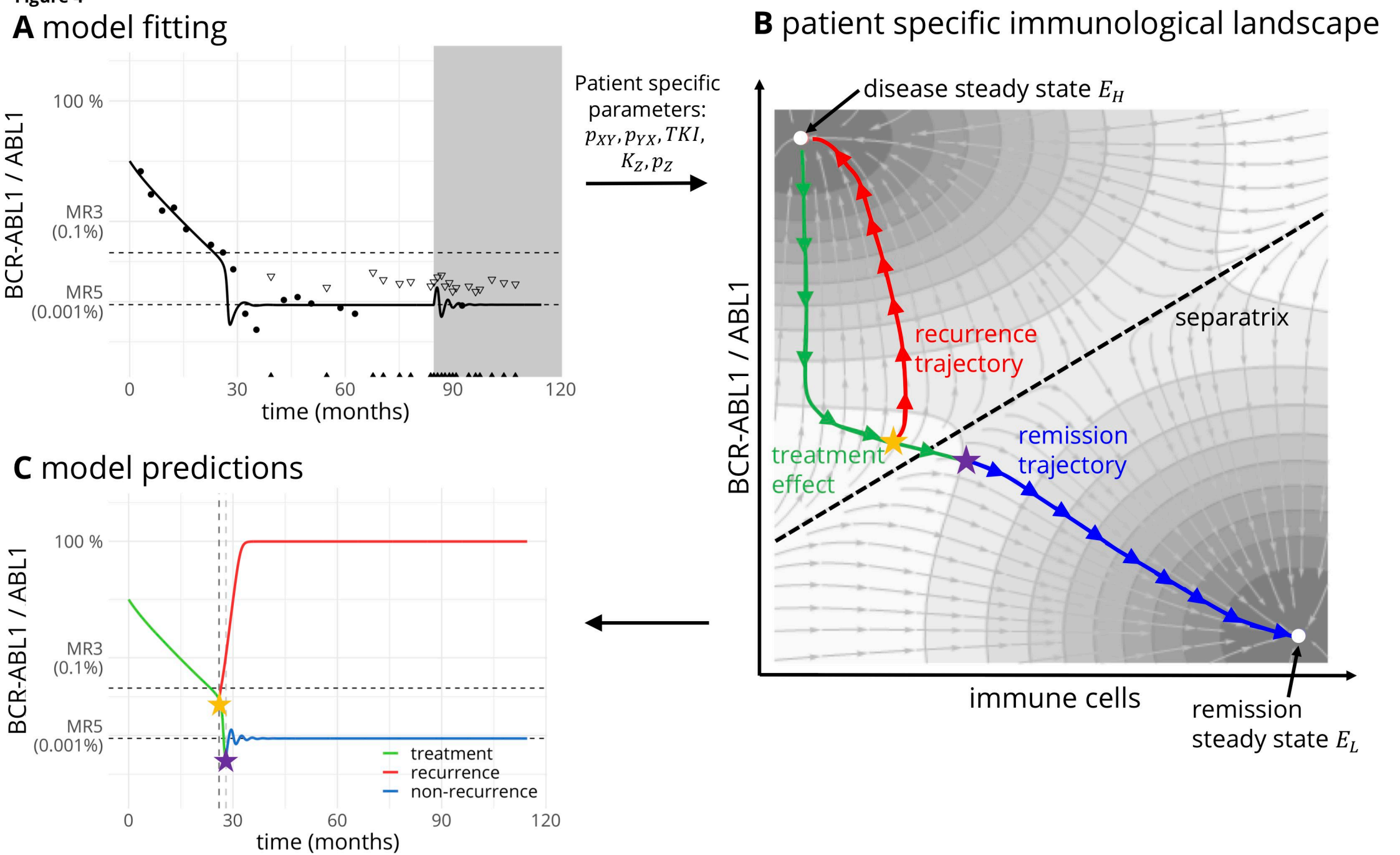
A model fitting
100 %
MR3
(0.1%)
MR5
(0.001%)
BCR-ABL1 / ABL1
0
30
60
90
120
time (months)
Patient specific
parameters:
$p_{XY}, p_{YX}, TKI,$
K_Z, p_Z
B patient specific immunological landscape
disease steady state E_H
recurrence
trajectory
separatrix
treatment
effect
remission
trajectory
BCR-ABL1 / ABL1
immune cells
remission
steady state E_L
C model predictions
100 %
MR3
(0.1%)
MR5
(0.001%)
BCR-ABL1 / ABL1
treatment
recurrence
non-recurrence
0
30
60
90
120
time (months)

Figure 5

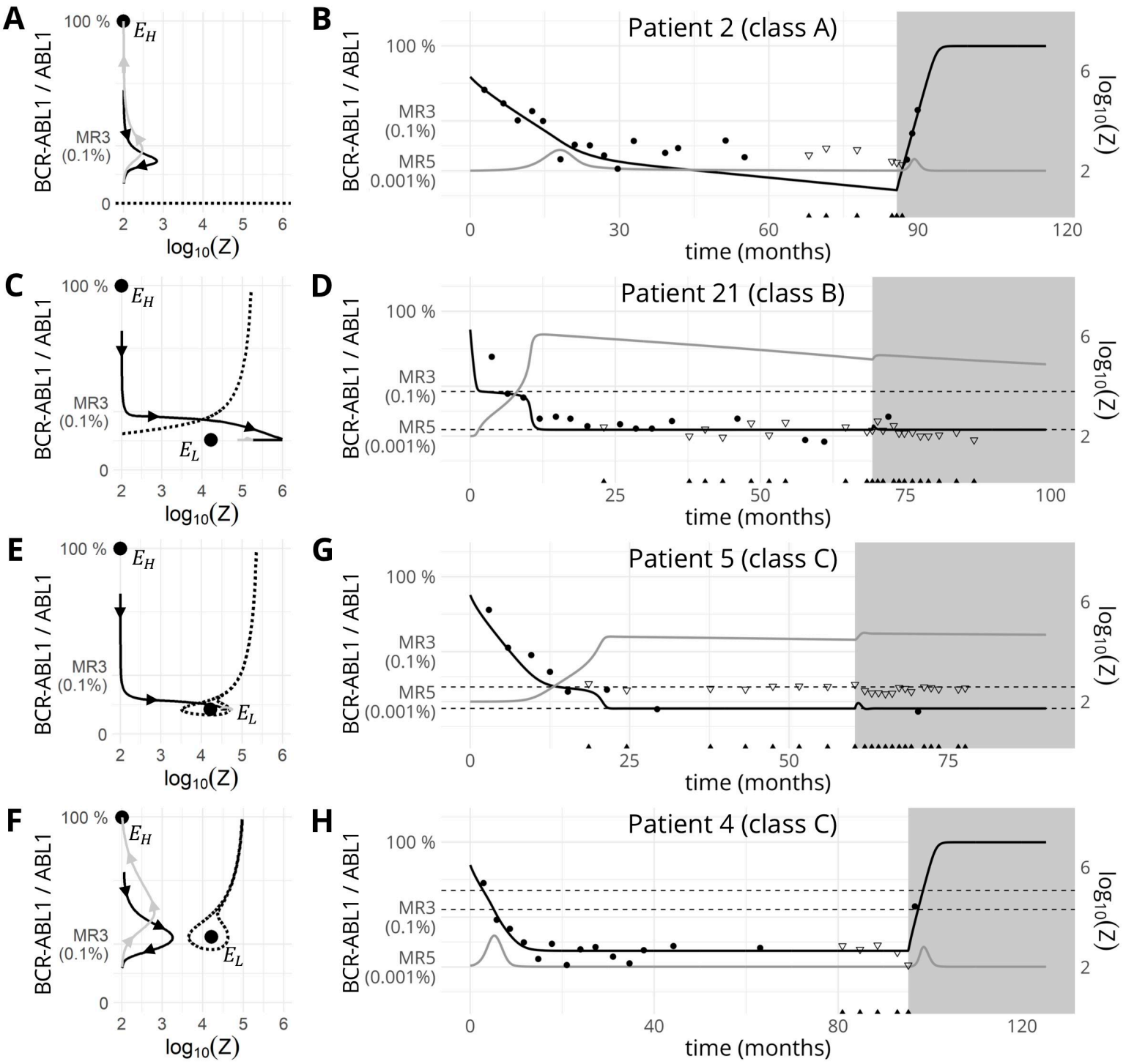
A
B
C
D
E
G
F
H
100 %
MR3
(0.1%)
0
E_H
E_L
BCR-ABL1 / ABL1
log10(Z)
Patient 2 (class A)
Patient 21 (class B)
Patient 5 (class C)
Patient 4 (class C)
MR5
0.001%)
time (months)

Figure 6

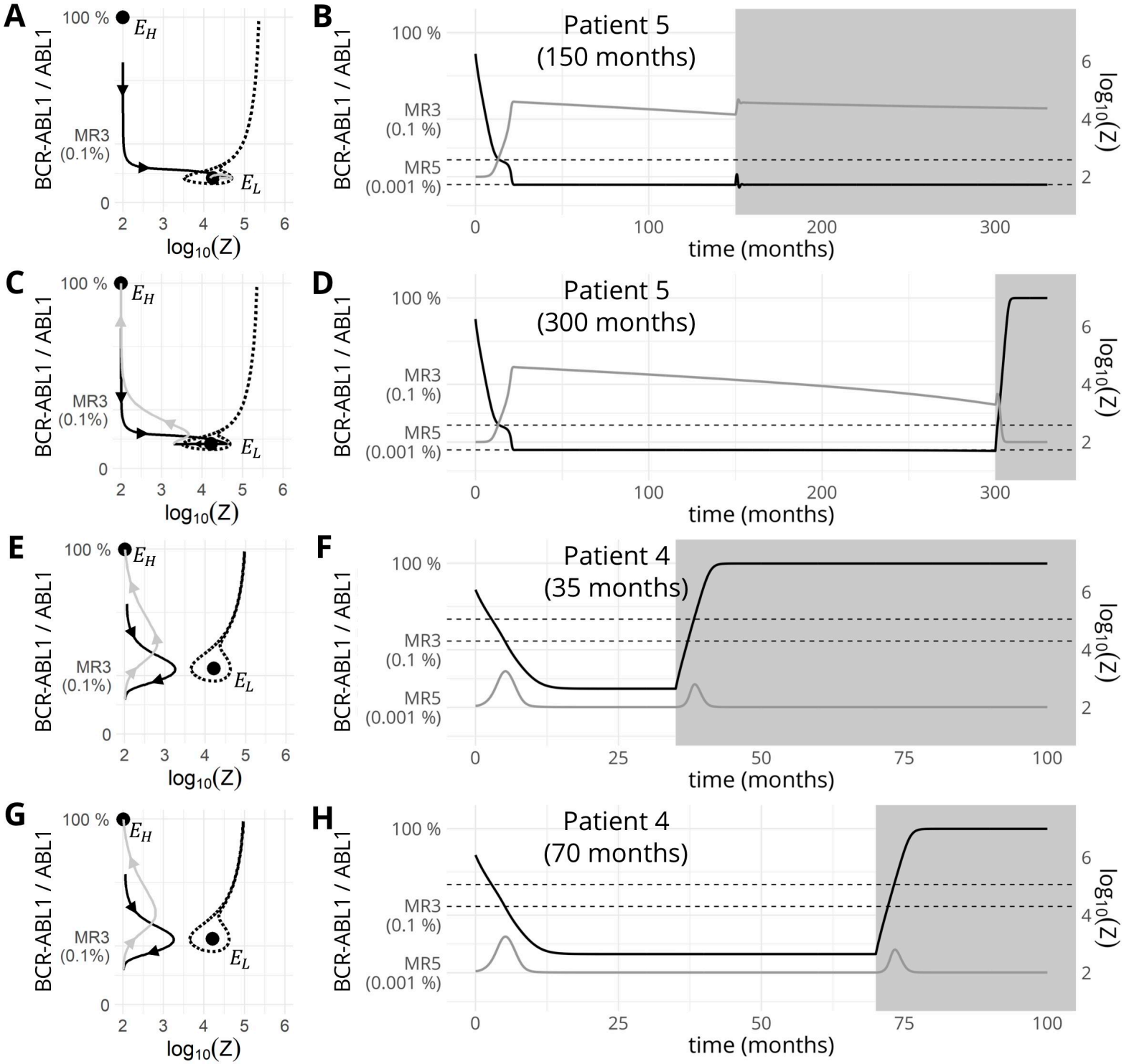
A
B
C
D
E
F
G
H
100 %
E_H
E_L
MR3
(0.1%)
0
BCR-ABL1 / ABL1
$\log_{10}$(Z)
2
3
4
5
6
Patient 5
(150 months)
Patient 5
(300 months)
Patient 4
(35 months)
Patient 4
(70 months)
MR3
(0.1 %)
MR5
(0.001 %)
0
100
200
300
25
50
75
time (months)
$\log_{10}$(Z)

Figure 7

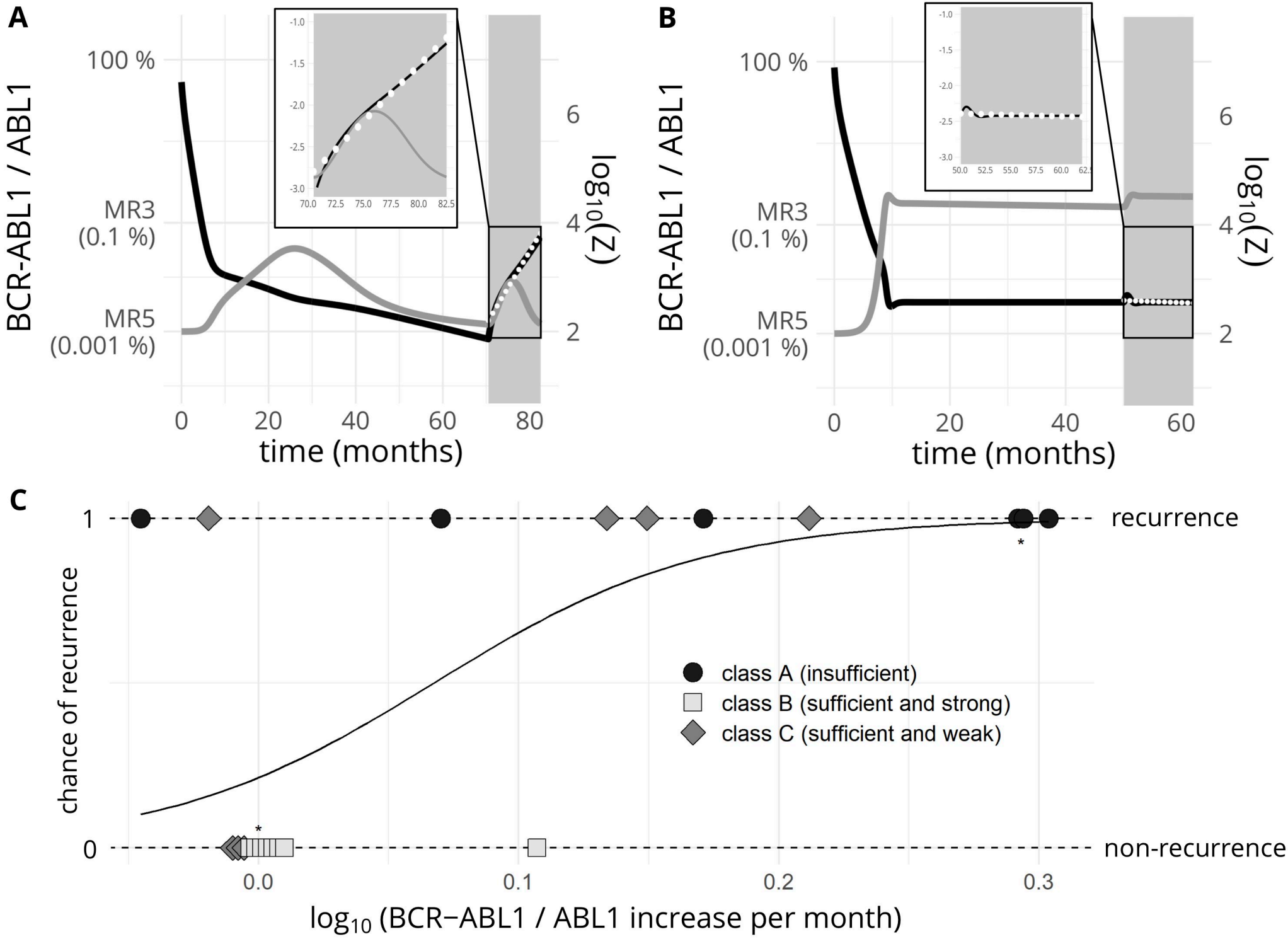
A
100 %
MR3
(0.1 %)
MR5
(0.001 %)
BCR-ABL1 / ABL1
log10(Z)
time (months)
B
C
recurrence
non-recurrence
chance of recurrence
class A (insufficient)
class B (sufficient and strong)
class C (sufficient and weak)
log10 (BCR−ABL1 / ABL1 increase per month)